This article has been accepted for publication in a future issue of this journal, but has not been fully edited. Content may change prior to final publication. Citation information: DOI 10.1109/ACCESS.2021.3135138, IEEE Access

IEEE Access
Multidisciplinary | Rapid Review | Open Access Journal

Date of publication xxxx 00, 0000, date of current version xxxx 00, 0000.

Digital Object Identifier 10.1109/ACCESS.2017.Doi Number

Test setup design for measuring the conductance in the mechanical part of Hybrid-Circuit-Breakers before and after current commutation

Dirk Bösche, Patrick Vieth, Frederik Anspach, Enno Peters, Ernst-Dieter Wilkening, Michael Kurrat, Member, IEEE

Technische Universität Braunschweig; Institute of High Voltage Technology and Electrical Power Systems; Braunschweig, Germany

Corresponding author: Dirk Bösche (e-mail: d.boesche@tu-braunschweig.de).

We acknowledge support by the Open Access Publication Funds of Technische Universität Braunschweig.

ABSTRACT The number of devices either providing or demanding direct current is growing more and more. This led to the renascence of DC grids and revealed a need for research. One critical component is the DC circuit breaker. It has to handle nominal and fault currents to keep the grid stable and operable. Interrupting currents in DC grids can be challenging because of the absence of a natural current zero crossing. Therefore, complex arcing chambers are needed. Especially at low currents, the self-induced force may not be sufficient to force the arc into the arcing chamber. Hybrid circuit breakers (HCB) are one possible solution to meet theses sophisticated requirements. There are several different topologies. All have in common that mechanical switches and semiconductors are combined to create a switch with the advantages of both technologies. One simple solution consists of two mechanical switches and one bypassing semiconductor circuit. The arc is used to achieve commutation from the mechanical to the semiconductor branch. While it carries the current, the mechanical switch regains its dielectric strength. Since this recovery time is short, the semiconductor can be overloaded within the limits of its thermal capacity. Defining the recovery time can be challenging. In addition, the effect of contact distance, arcing time and current value are unknown.

To research the recovery behavior a model-switching chamber with an adjustable contact gap is developed. This device under test (DUT) was implemented into a test circuit that reproduces part of the hybrid switching process. When the arc between the contacts of the DUT reaches its steady state, a parallel commutating path is activated. The residual conductance of the decaying arc was measured. The development and several iteration steps of the test circuit and DUT are laid out. Finally, some test runs and initial measurements are presented.

INDEX TERMS arc conductivity, dielectric recovery, direct current, hybrid DC circuit breaker, recovery behavior, test circuit development

I. INTRODUCTION

The growing numbers of DC-applications result in a higher demand on DC-switchgear to ensure safe operation [1] [2]. Low inductances in DC-Grids cause high and fast rising fault currents. In consequence, a sufficient switching speed is required [3]. Mechanical DC circuit breakers often use the self-induced Lorentz force to lead the arc in a quenching chamber. At low currents, the resulting force is small resulting in slow, sometimes insufficient arc movement. The result might be a switching off failure, which can cause further damage to the switch or the whole system [4]. By enhancing a mechanical switch with power electronics (PE) the switch can be enabled to interrupt those currents. This so-called Hybrid-circuit-breaker (HCB) is able to achieve fast switching and minimizes contact erosion [5] [6]. This combination of mechanical circuit breaker and power electronic components might be the ideal switch in future DC grids [7].

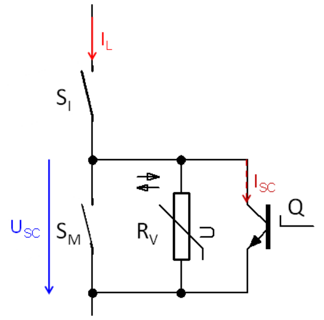

Fig. 1. **Example of a hybrid circuit breaker**

Depending on the topology of the HCB, current commutation from the mechanical to the semiconductor switch can be achieved by an arc or with additional components. This arcless commutation is often realized with semiconductors in series with the mechanical switch [3] [8] [9]. However, it is possible to use the arc to charge a capacitor, which then powers the electronic. In this case, no additional external supply is needed [5] [10]. The required arc voltage for complete commutation depends among others on the used semiconductors, contact material and load current. The arc voltage can be raised by increasing the switching gap. Depending on the used mechanical switch, the PE has to conduct the current for several 100 µs. This ensures that the mechanical switch regains a sufficient dielectric strength. Otherwise, it might not withstand the recovery voltage, which will lead to an arc reignition. The time needed depends on the deionization processes in the chamber. By measuring the conductance of the decaying arc plasma, a minimum activation time for the PE can be defined. Thus, allowing a switching performance optimization. [5] [11]

A basic setup of a HCB can be seen in Fig. 1. It consists of the insolation switch S_I, the main switches S_M, an IGBT Q and a Metal Oxide Varistor R_V [5]. The switch off process will be explained subsequently using Fig. 2. It can be split up into five different phases. The switch S_I ensures galvanic separation and switches currentless. Therefore, S_1 can be neglected in the explanation of the current breaking process.

1) CONDUCTING

Initially the load current I_L flows through the main switch S_M. This ensures minimal conduction losses.

2) ARCING

At t_1 the switch S_M is opened and an arc forms between the contacts causing a voltage jump. The voltage slowly increases because of the contacts moving apart. The longer the timeframe the larger the contact distance when the next phase is initiated. Furthermore, the arc can be used to draw energy to power an electronic, which controls the IGBT Q [5] [10]. To minimize contact erosion arcing time should be as short as possible.

3) RECOVERING

At the time t_2 the IGBT Q is turned on. Its forward voltage is significantly lower than the arc voltage, which forces the current to commutate from the mechanical switch S_M onto the semiconductor branch with the IGBT Q. The commutation time depends among others, on the commutation inductance, the instantaneous current and the resulting voltage drop caused by the semiconductor. Commonly this process takes several µs [5] [12]. The arc between the contacts of S_M will extinguish as soon as the

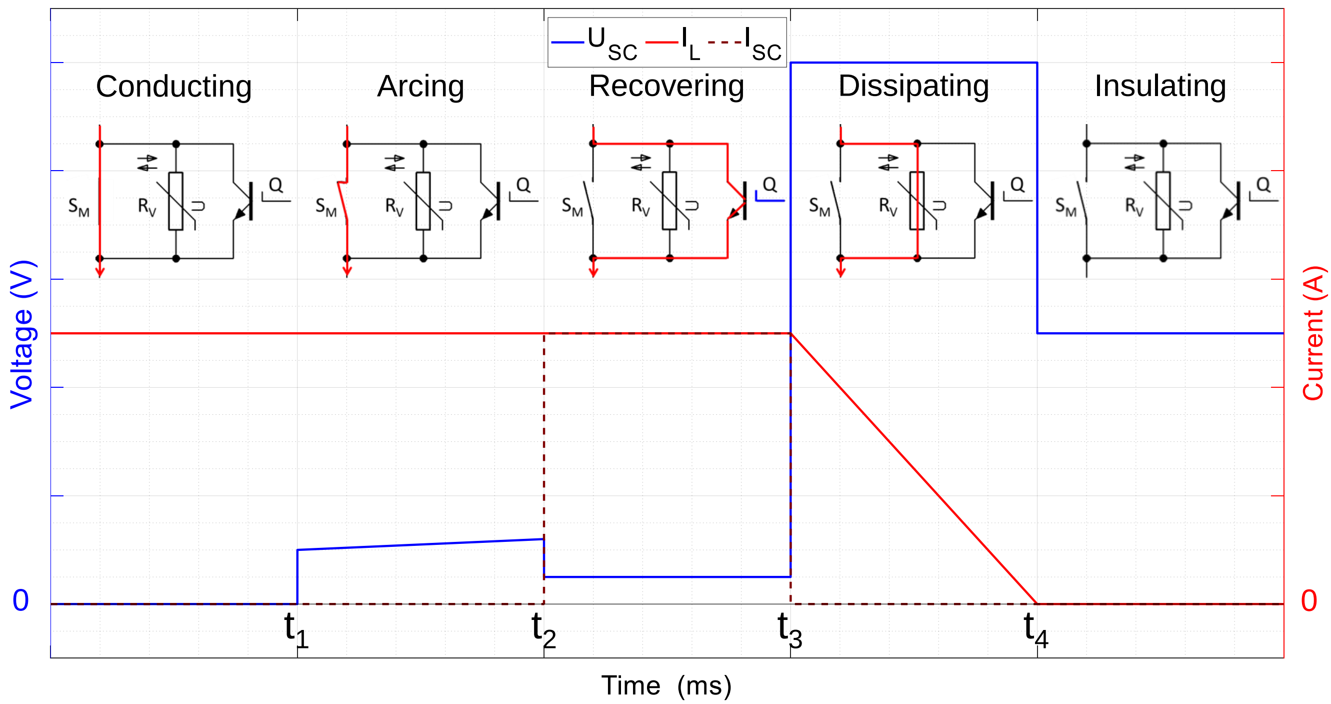

Fig. 2. **Overview of the current breaking process**

This article has been accepted for publication in a future issue of this journal, but has not been fully edited. Content may change prior to final publication. Citation information: DOI 10.1109/ACCESS.2021.3135138, IEEE Access

current through the switch has become zero. However, the conductivity of the residual arc column cannot change instantaneously, because the plasma retains its thermal energy. Therefore, the IGBT Q has to carry the load current for a certain amount of time to allow the plasma to cool down. This ensures that the switch S_M can reach a sufficient dielectric strength to prevent the arc from reigniting during phase 4. In [13] the authors describe an efficient determination of the minimal conduction time of the semiconductor branch. It is possible to overload the IGBT without damaging it. However, conduction time has to be kept short because the thermal capacity of the semiconductor is rather limited [14].

4) DISSIPATING

At t_3 the IGBT Q is turned off. This forces the current to commutate onto the varistor, which limits the overvoltage due to a nonlinear U, I characteristics. It dissipates the inductive stored energy and forces the current to become zero. The overvoltage has to be kept below the maximum blocking voltage of the IGBT for all load currents. A lower overvoltage reduces stress on the switching gap and the IGBT but increases total switching time [5].

5) INSULATING

At t_4 the current has become zero and the isolating switch can open currentless and ensure a galvanic separation.

To investigate the switching gap recovery a simple mechanical switch was created in [15]. After contact separation, the current was switched off and a test voltage applied onto the gap. The results were evaluated using a Weibull-Estimation. One major drawback of this setup is that the exact contact distance is unknown when the test voltage is applied. Moreover, the development of the plasma conductivity is not recorded. No reliable statements about the dielectric recovery could be made.

A new test setup was developed to investigate the recovering phase of the current breaking process of a hybrid switch. The changing conductance of the residual arc column can be recorded to estimate the minimal conduction time of the semiconductor branch. The influence of contact distance and current level onto the recovery behavior is particular of interest. Therefore, a model-switching chamber with an adjustable contact gap was designed. The development process and setup iterations are presented and evaluated. The final test circuit can easily be adapted to investigate different protection devices.

II. Basic design considerations

Fig. 3 shows the basic design considerations of the test circuit. The function of the elements will be explained subsequently.

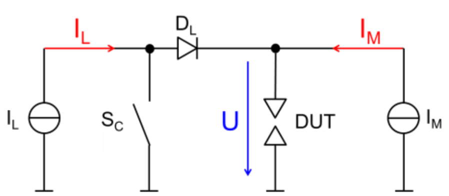

Fig. 3. **Basic test circuit setup**

This test circuit reproduces the first three phases of the described current breaking process (Fig. 2). All elements of the hybrid circuit breaker can be identified with the absence of the varistor. It is not needed, because of the lack of the dissipating phase. The device under test (DUT) replaces the main switch S_M and the commutation switch S_C replaces the IGBT Q.

Initially the load current I_L is flowing through the connected electrodes of the *DUT* (conducting phase). Then the arc is ignited and burns for a specific amount of time (arcing phase). The current commutates when the switch S_C is closed. The arc extinguishes and the plasma of the residual arc column can cool down (recovering phase). To measure the decaying arc conductance an additional measurement current I_M needs to flow through the *DUT*. It has to be small in order to keep the energy input into the residual arc low. Otherwise, the current would affect the recovering process. The Diode D_L prevents the measurement current from flowing through the switch S_C.

The device under test (DUT) consists of two opposing electrodes without any chamber walls to ensure a free-burning arc. They can be changed easily to allow different materials to be tested. The contact gap can be set in 1 mm increments from 1 mm up to a total distance of 20 mm. The exact setup will be explained later in the manuscript.

A. *Test Setup A*

Derived from this basic design consideration, the test setup A as shown in Fig. 4 was designed. The data of each component is mentioned in the final test circuit, which is explained in subsection *D* in detail.

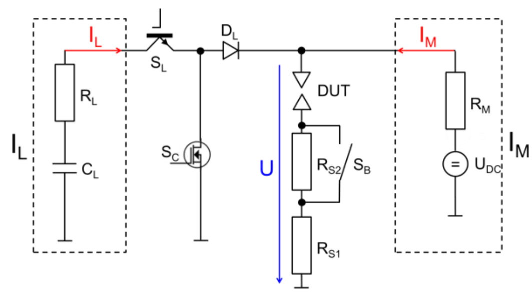

Fig. 4. **Test setup A**

The load current source is realized using the capacitor C_L and the resistance R_L. The precharged capacitor provides the current, which is limited by the resistor. The load current can be switched on or off using the IGBT S_L. The commutation switch S_C will be composed of several in series and parallel connected MOSFETs to create a fast close to ideal switch.

The voltage source U_{DC} provides the measuring current I_M, which is limited by the resistor R_M. Since I_L is several magnitudes larger than I_M, two shunts R_{S1} and R_{S2} are implemented to record both currents with sufficient resolution. The large shunt R_{S2} is used to measure the small current I_M. To prevent R_{S2} from influencing the test and taking damage, it should be bypassed as long as the load current is applied onto the *DUT*. Therefore, the bypassing switch S_B was added.

This article has been accepted for publication in a future issue of this journal, but has not been fully edited. Content may change prior to final publication. Citation information: DOI 10.1109/ACCESS.2021.3135138, IEEE Access

Two possible bypass switch solutions are shown in Fig. 5 and discussed subsequently.

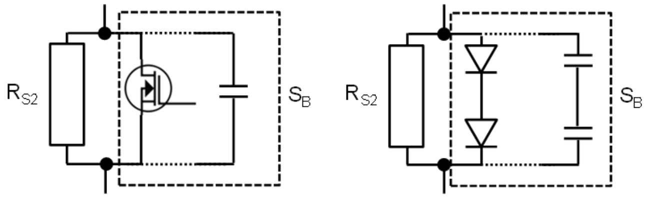

A: active switch B: passive switch

Fig. 5. **Possible shunt bypass solutions**

1) ACTIVE SWITCH

Low voltage MOSFETs are readily available. They offer minimal on state losses and fast switching. Taking a closer look at more than 40 datasheets, the junction capacity varies from about 500 – 3500 pF. Since several MOSFETs have to be connected in parallel, their capacity will act as a high pass negatively influencing the measurement. In addition, the synchronization of control signals to the test sequence is a challenging task. If switched off while conducting the load current the switch may be damaged.

2) PASSIVE SWITCH

Diodes conduct only a significant amount of current if the applied voltage is above their diffusion voltage. This characteristic can be used to build a passive bypass. At a certain voltage level across the shunt, the diodes start conducting and therefore limit the current flowing through the shunt. Measuring the junction capacitance of nine fast switching diodes showed a range of about 150 – 500 pF. The resulting capacity of the bypass can be reduced if several diodes are connected in series. This raises the activation voltage, which increases the stress on the shunt. In addition, the losses are high compared to the active switch. The temperature of the diodes increases when bypassing the load current. A junction temperature rise will decrease their diffusion voltage. To evaluate this passive bypass a simple test was carried out. The Results are illustrated in Fig. 6.

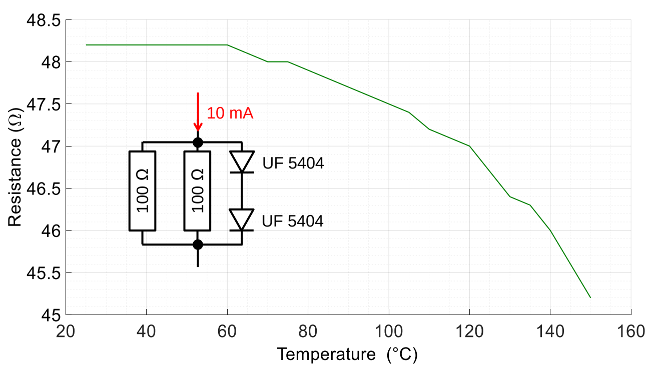

Fig. 6. **Resulting resistance of the bypass solution B at various temperatures**

A constant current of 10 mA is applied onto a circuit consisting of two series connected diodes in parallel with two parallel resistors. The diodes were mounted to a heating source and the voltage recorded. The resulting shunt resistance of this setup starts to change at temperatures higher than 60 °C. To prevent heating up, several diodes have to be connected in parallel. This will increase the resulting capacity of the setup, which will falsify the measurement when recording transients.

Considering the disadvantages of both concepts, bypassing the shunt does not seem like a viable solution. Therefore, measuring the currents in different branches is investigated.

B. Test Setup B

To avoid the prior mentioned downsides of bypassing R_{S2}, the shunt is moved to the measuring current branch. The resulting test circuit can be seen in Fig. 7

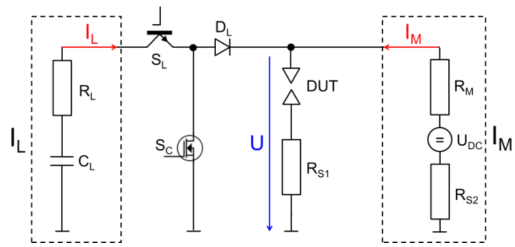

Fig. 7. **Test setup B**

The shunt R_{S1} measures the current, which flows through the DUT during arcing phase (see Fig. 2). When the commutation switch S_c is activated, the load current is shortened. The Diode D_L blocks the measuring current forcing it to flow through the *DUT* only. Therefore, under these conditions the current can be recorded with R_{S2} in the source branch of I_M. However, this is only possible if the reverse current through the Diode is negligible. Therefore, the device must be carefully selected and the static and dynamic behavior has to be investigated.

The static reverse current of a diode is strongly affected by the junction temperature. Conducting the load current will cause heating up. Therefore, it is important to know how the temperature affects the reverse current of the used device. Several diodes are investigated. The results of two examples are plotted in Fig. 8.

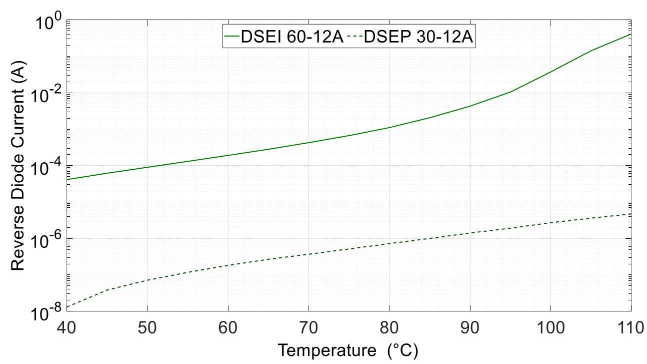

Fig. 8. **Reverse diode current at different temperatures**

The investigated diode is mounted to a heating source and a reverse voltage of 1 kV was applied. A 100 kΩ resistor limits the maximum current. Voltage across the diode and the current is recorded. The resulting reverse

IEEE Access
Multidisciplinary ⋮ Rapid Review ⋮ Open Access Journal

current is extrapolated, as if no limiting resistor is in the circuit.

The reverse current of the diode DSEI 60-12A starts at about 40 µA and increases with rising temperature. The diode DSEP 30-12A starts at a much lower current of about 10 nA and stays below the starting current of the diode DSEI 60-12A over the entire recorded temperature range. The diode DSEP 30-12A ensures significantly low reverse current even when heating up. However, since the current increases exponentially connecting several diodes in parallel to minimize heating up seams viable. Ten diodes are connected in parallel to realize the diode D_L. In series to each diode is a 50 mΩ balancing resistor, which ensures equal current, sharing.

The composed diode forms a parasitic capacity allowing transient reverse currents to pass. This current has to be subtracted from the measuring current I_M in order to receive the current flowing through the *DUT*. In addition, the capacity of D_L changes with the applied reverse voltage. The resulting capacity was measured while different reverse voltages where applied. The results are shown in Fig. 9.

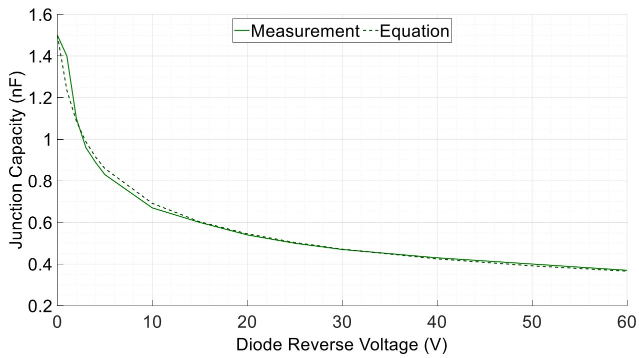

Fig. 9. **Junction capacity C_J of the Diode D_L at different reverse voltages**

The results are used to estimate the parameters necessary for the following equation [16]:

$$C_J = \frac{C_{J0}}{\left(1 + \frac{U_R}{V_J}\right)^M}$$

The MATLAB curve fitting toolbox was used to find the values given in TABLE I.

TABLE I. RESULTING APPROXIMATION PARAMETERS

C_{J0}	V_J	M
1.5 nF	1.5 V	0.38

Closing the commutation switch S_C will effectively connect the diode D_L in parallel with the *DUT*. Therefore, the recorded voltage U is almost equal to the reverse voltage of the Diode D_L. Only the small voltage drop caused by the load current flowing through S_C has to be subtracted. However, this effect will minimize with raising voltage U and can therefore be neglected. Since voltage and capacity are known, the resulting transient reverse current can be calculated. In return, the result and the measured current I_M can be used to calculate the current through the *DUT*.

C. Test Setup C

The contacts of the *DUT* are preset to a fixed distance. The arc ignition is realized with a thin copper wire between the electrodes. It has to be vaporized by an initial current. Afterwards the resulting arc has to be supplied with sufficient power to remain stable until the actual test is carried out. Therefore, the test setup was extended as pictured in Fig. 10.

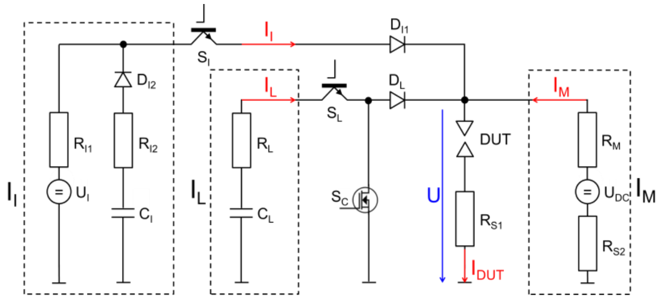

Fig. 10. **Test setup C**

The value and task of each device of the initial circuit can be seen in TABLE II.

TABLE II. COMPONENTS INITIAL CIRCUIT

Symbol	Task	Value
U_I	Maintaining the initial arc	500 V
	Precharged to U_I	
C_I	Delivers the current to vaporize the copper wire	2.5 mF
R_{I1}	Current limiting	100 Ω
R_{I2}	Current limiting	20 Ω
S_I	Connects and disconnects the initial circuit	5SNA 1200G330100
D_{I1}	Blocking I_M	DSEP 30-12A
D_{I2}	Blocking maintaining current	DSEP 30-12A

One example of a complete test sequence can be seen in Fig. 11. The gap distance of the DUT was set to 10 mm.

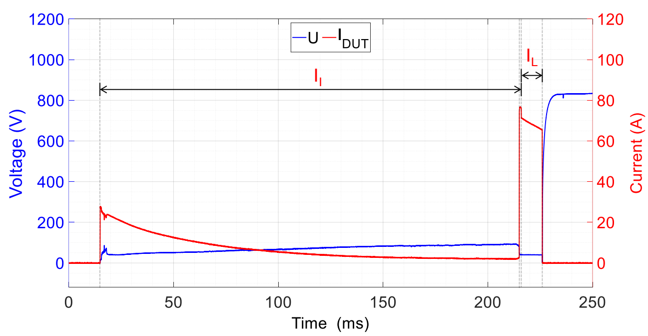

Fig. 11. **Initial and test sequence**

At the beginning, S_I is closed and the current flows through the copper wire. The initial current is about 25 A. It is mostly provided by the precharged capacitor C_I. The

This article has been accepted for publication in a future issue of this journal, but has not been fully edited. Content may change prior to final publication. Citation information: DOI 10.1109/ACCESS.2021.3135138, IEEE Access

copper wire vaporizes after a few ms and the arc ignites between the electrodes. The current decreases due to the discharging capacitor C_I. To cover the energy demand of the arc, the voltage increases slightly. The initial current flows for 200 ms to reach a steady state. With the closing of S_L, the actual test begins. The arcing and recovery phase of six measurements can be seen in detail in Fig. 12.

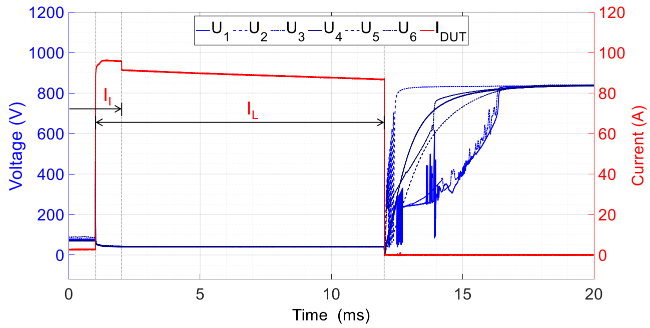

Fig. 12. **Reproducibility of the test setup using a copper wire for arc ignition**

The initial current I_I and the load current I_L superpose for 1 ms. To ensure a steady state of the arc, the load current is applied for 10 ms. Then the switch S_C is activated which causes rapid commutation of the load current. The voltages rise to the value set by the Source U_{DC}. The characteristics of each of these six recovery voltages differ although their load currents match closely.

Taking a closer look at the anode of the electrodes in Fig. 13, a major drawback of the ignition variant becomes obvious.

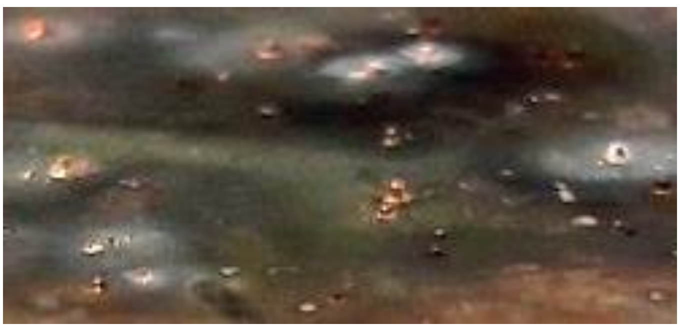

Fig. 13. **Anode after about 30 ignitions with various load currents**

The ends of the wires weld onto the copper electrode. The alteration of the contact surface may be one reason for the inconsistencies in the measurement. In addition, for each test, the arc forms at different locations. The roots of anode and cathode may not oppose each other leading to different arc length.

Arc ignition via copper wire ads significant drawbacks for the test run. Placing the wire between the contacts takes a huge amount of time, because the whole test setup has to be shut down. Frequently the wire was placed incorrectly. It either made no or too much contact so that no arc could be ignited. Therefore, the *DUT* and test setup were revised.

D. Test Setup D

The experimental setup and *DUT* were enhanced to eliminate the ignition via copper wire to evade the problems mentioned earlier. Therefore, the experimental setup simplifies as pictured in Fig. 14.

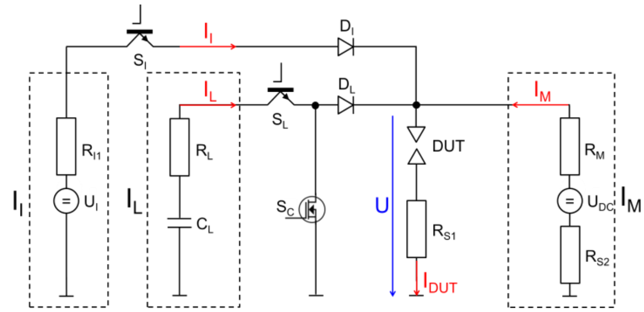

Fig. 14. **Test setup D**

The circuit is almost identical to the test setup C, but the dedicated devices to vaporize the copper wire are gone. The arc ignition is accomplished by making the upper electrode movable. The value and task of each device of the final circuit can be seen in TABLE II.

TABLE III. COMPONENTS FINAL CIRCUIT

Symbol	Task	Value
U_I	Maintaining the initial arc	500 V
R_{I1}	Current limiting	100 Ω
S_I	Connects and disconnects the initial circuit	5SNA 1200G330100
D_I	Blocking I_M	DSEP 30-12A
C_L	Precharged to 450-500 V Delivers the load current	21 mF
R_L	Current limiting	2-85 Ω
S_L	Connects and disconnects the load circuit	5SNA 1200G330100
D_L	Blocking I_M	10 parallel strings DSEP 30-12A with 50 mΩ balancing resistor
S_C	Current commutation to simulate the transition from phase 2 to phase 3 of the hybrid switch off process	3 serious modules consisting of 14 parallel MOSFETs IRFP4668
DUT	Device Under Test	
R_{S1}	Measuring the load current	coaxial measurement shunt 10 mΩ
R_M	Current limiting	100 kΩ
U_{DC}	Delivering the measuring current	1 kV
R_{S2}	Measuring the measuring current	coaxial measurement shunt 100 Ω

At the beginning of the test sequence, both electrodes are touching. The switch S_I is closed and a current of about 5 A begins to flow. The upper electrode is moved upwards. As the contacts separate, an arc is forming between the contacts. The arc is powered by the source U_I until the end position of the upper electrode is reached and the load current is switched on. Identical to the prior test sequence, the initial and load current superpose for 1 ms. The load-conducting phase of the arc and the resulting recovery voltages of ten measurements at a switching gap of 10 mm are plotted in Fig. 15.

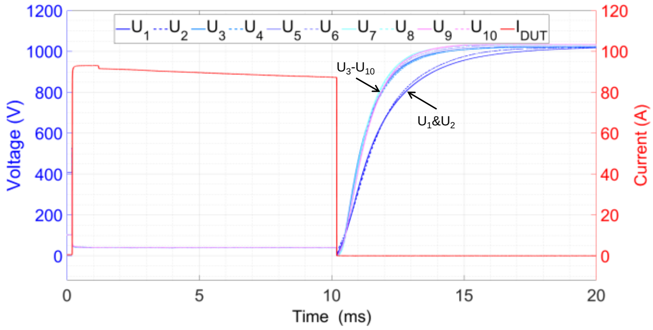

Fig. 15. **Reproducibility of the test setup using movable contacts for arc ignition**

Comparing the results with those generated by arc ignition via copper wire (Fig. 12), the much better reproducibility can be seen. Only the first two tests show a slightly different recovery voltage behavior.

III. Device under test

Fig. 16 shows the side view of the *DUT* in its final form. The first version had two identical electrodes with flat contacts surfaces. Due to the changing arc ignition system, the upper contact plate had to be redesigned.

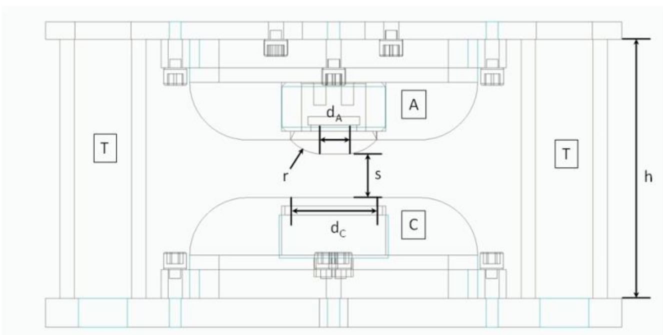

Fig. 16. **Technical drawing of the DUT**

The upper and lower electrodes contain the contacts and unify the electric field. Otherwise, the arc would have an affinity to move towards high spots. Since the arc only burns between the contacts, the electrodes can be made out of aluminum. The contacts are made out of copper and can be changed easily to test different materials in future researches. A screw presses the lower contact in. The upper contact is hold in a clamp fixed to a movable rod. The contact has a conical rim to ensure proper alignment when reaching upper end position. Several contact shapes have been tested until the used was found. It ensures that the arc stays between the flat parts of the contacts even at a switching gap of 10 mm.

The height of the switching gap can be set by changing the tube spacers. Several rings of different thicknesses can be stacked to reach the desired height.

The relevant dimensions of the *DUT* are listed in TABLE IV.

TABLE IV. DIMENSIONS OF DUT

Symbol	Description	Value
A	Upper electrode	Anode
C	Lower electrode	Cathode
T	Tube spacers to set the distance of the switching gap	75 – 95 mm
d_A	Diameter anode contact	7.65 mm
d_C	Diameter cathode contact	30 mm
S	Contact gap	0 – 20 mm
r	Rounding upper electrode	15 mm

Different from the actuation in a switch, the speed of the moving contact is not of interest. Therefore, a simple and cheap actuator to lock and unlock car doors was used. A 3D model of the *DUT* is presented in Fig. 17.

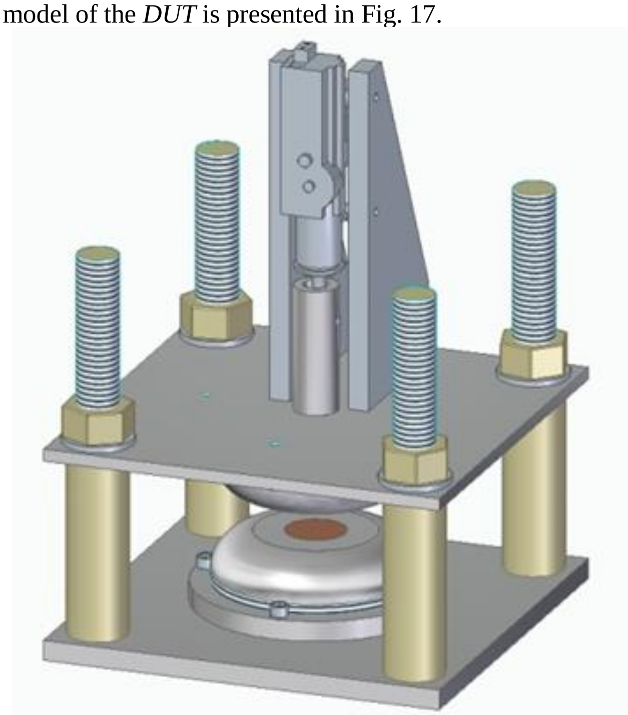

Fig. 17. **3D view of the DUT**

IV. Initial Measurement results

Some initial measurements with the final setup were carried out. The switching gap was set to 10 mm and the load current to 200 A. For the first investigations, the contact material was chosen to be copper. The arc resistance was calculated using the currents measured by R_{S1} and R_{S2} as well as the voltage *U* recorded via a 1:100 measuring probe. The resulting arc resistance is plotted in Fig. 18.

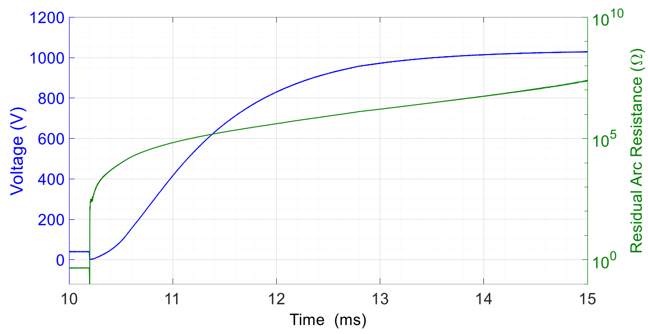

Fig. 18. **Measured resistance of the decaying arc plasma**

A few µs after the 10 ms mark, the switch S_C is activated and the load current commutates which takes about 5 µs. Initially the current recorded by R_{S1} is used to calculate the arc resistance. This changes when the measured value of I_L is equal or below the value of I_M for the first time. This indicates that the commutation process has been completed. Therefore, after this point in time I_M is used to calculate the residual arc resistance.

As long as the load current is flowing completely through the arc, its resistance remains low. It changes rapidly with the beginning of the commutation process. However, during this interval measuring accuracy is limited by the fast transients causing disturbances as well as the hard switch between the signals used for calculation. This initial rapid increase slowly changes to become almost exponential. Therefore determining the time necessary for the switch to regain its dielectric strength can be achieved. However, this is only possible if the minimal residual arc resistance that surly prevents any reforming of a stable arc at a given recovery voltage is known.

V. Conclusion

Due to the increasing interest in DC grids, a rising demand in suitable switches can be identified. One particular suitable technological approach is the HCB. Several setups have been presented in different publications. One solution uses the arc itself to achieve commutation from the mechanical to the semiconductor switch. The current is carried for an amount of time to ensure, that the switching gap can re-establish its dielectric strength. However, defining this time can be quite challenging. If it is too long, unnecessary stress is put onto the semiconductor. If it is too short, the arc may reignite.

To investigate the influence of the gap properties onto the arc decay a test circuit was developed. The incremental development steps and design considerations were laid out. The circuit reproduces the crucial part of the hybrid switch off process and allows the residual arc to be measured. The arc ignition was optimized to improve on the reproducibility. The switching gap distance can be set in a range of 0 – 20 mm. In addition, the contacts can easily be replaced. Therefore, different materials may be investigated in the future.

REFERENCES

[1] H. Wirth, „Aktuelle Fakten zur Photovoltaik in Deutschland,“ Frauenhofer ISE, 2021.

[2] S. e. a. Michaelis, „Roadmap Batterie-Produktionsmittel 2030, Update 2020,“ VDMA Batterieproduktion, Frankfurt am Main, 2020.

[3] C. Meyer, M. Kowal und R. W. Doncker, „Circuit breaker concepts for future high-power DC-applications,“ Piscataway, NJ, IEEE Service Center, 2005, p. 860–866.

[4] H.-C. Köpf, Schalten von Gleichströmen in automobilen HV-Bordnetzen bis 500 V, unter Berücksichtigung der Lichtbogenwanderung im Doppelkontaktsystem, Braunschweig: Dr. Hut, München, 2019.

[5] D. Bösche, E.-D. Wilkening, H. Köpf und M. Kurrat, „Hybrid DC Circuit Breaker Feasibility Study,“ *IEEE Transactions on Components, Packaging and Manufacturing Technology,* Bd. 7, Nr. 3, p. 354–362, 2017.

[6] L. C. E. -D. W. M. K. F. Anspach, „Overview about different 500 V low voltage DC-Switchgear topologies and comparison of their switch off performance,“ in *VDE High Voltage Technology*, 2020.

[7] F. A. E. -D. W. a. M. K. L. Claaßen, „Investigation of a Mechanical Switch within a Hybrid Circuit Breaker for Protection in DC Grids,“ in *IEEE 66th Holm Conference on Electrical Contacts and Intensive Course (HLM)*, 2020.

[8] H. Xiao, Z. Xu, L. Xiao, C. Gan, F. Xu und L. Dai, „Components Sharing Based Integrated HVDC Circuit Breaker for Meshed HVDC Grids,“ *IEEE Transactions on Power Delivery,* Bd. 35, Nr. 4, p. 1856–1866, 2020.

[9] D. Jovcic, M. Zaja und M. H. Hedayati, „Bidirectional Hybrid HVDC CB with a single HV Valve,“ IEEE, 822020, p. 1.

[10] D. W. E. K. H. Bösche, „DISCONNECTOR FOR GALVANIC DIRECT CURRENT INTERRUPTION“. EU Patent EP15756858, 2016.

[11] M. Lindmayer, Hrsg., Schaltgeräte, Berlin: Springer, 1986, p. 250.

[12] S. Greitzke, Untersuchung an Hybridschaltern, Braunschweig: Technische Universität Braunschweig, 1988.

[13] F. Anspach, P. Vieth, D. Bösche, L. Claaßen, E.-D. Wilkening und M. Kurrat, „Presentation of a novel and laboratory proved method to determine efficiently the minimum deionization time in hybrid cicuit breaker,“ IEEE, San Antonio, 2021.

[14] B. H. Bünsow, Verhalten von 600V NPT-IGBT Modulen 2. und 3. Generation bei Stoßbelastungen, Braunschweig: Dr. Hut, 2015.

[15] M. A. M. H. M. K. D. Bösche, „INVESTIGATION OF THE RECOVERY BEHAVIOUR OF A SMALL,“ in *Plasma Physics and Technology*, Prague, 2017.

[16] P. Baumann, Parameterextraktion bei Halbleiterbauelementen, Bremen: Springer Vieweg, 2019.